Computer-Aided Detection for Prostate Cancer Detection based on Multi-Parametric Magnetic Resonance Imaging

Guillaume Lemaître*, Robert Martí†, Mojdeh Rastgoo*, Fabrice Mériaudeau‡
*LE2I UMR6306, CNRS, Arts et Métiers, Univ. Bourgogne Franche-Comté,
12 rue de la Fonderie, 71200 Le Creusot, France
†ViCOROB, Universitat de Girona, Campus Montilivi, Edifici P4, 17071 Girona, Spain
‡Centre for Intelligent Signal and Imaging Research (CISIR), Electrical & Electronic Engineering Department,
Universiti Teknologi Petronas, 32610 Seri Iskandar, Perak, Malaysia
¶Corresponding author: fabrice.meriaudeau@utp.edu.my

***Abstract*—prostate cancer (CaP) is the second most diagnosed cancer in men all over the world. In the last decades, new imaging techniques based on magnetic resonance imaging (MRI) have been developed improving diagnosis. In practise, diagnosis can be affected by multiple factors such as observer variability and visibility and complexity of the lesions. In this regard, computer-aided detection and diagnosis (CAD) systems are being designed to help radiologists in their clinical practice. We propose a CAD system taking advantage of all MRI modalities (i.e., T_2-W-MRI, DCE-MRI, DW-MRI, MRSI). This system has been extensively tested on a dataset which has been made publicly available.**

***Index Terms*—Computer-Aided Diagnosis, Prostate Cancer, normalization, Multi-parametric MRI**

I. Introduction

Current prostate cancer (CaP) screening consists of three different stages. First, prostate-specific antigen (PSA) control is performed to distinguish between low- and high-risk CaP. To assert such diagnosis, samples are taken during prostate biopsy and finally analyzed to evaluate the prognosis and the stage of CaP.

Although PSA screening has been shown to improve early detection of CaP [1], its lack of reliability motivates further investigations using magnetic resonance imaging (MRI)-based computer-aided detection and diagnosis (CAD). Current research is focused on identifying new biological markers to replace PSA-based screening [2], [3], [4]. Until such research comes to fruition, these needs can be met through active-surveillance strategy using multiparametric MRI (mp-MRI) techniques [5], [6].

In a recent paper, Lemaitre et al. [7] reviewed around fifty papers recently published and focusing on CAD system for CaP. Most of the work reviewed could fit on the pipeline presented in [8]which consists of different steps: pre-processing, segmentation, registration, feature detection, feature balancing, feature selection/extraction, and finally classification. However, non of the reviewed work, except thisone used all the MRI modalities (T_2 Weighted (T_2-W), dynamic contrast-enhanced (DCE),diffusion weighted (DW) and magnetic resonance spectroscopy imaging (MRSI)) and only half of the studies were related to the central gland of the prostate.

II. Methodology

The mp-MRI data are acquired from a cohort of patients with higher-than-normal level of PSA. The acquisition is performed using a 3 T whole body MRI scanner (Siemens Magnetom Trio TIM, Erlangen, Germany) using sequences to obtain T_2-W-MRI, DCE-MRI, DW-MRI, and MRSI. Aside of the MRI examination, these patients also have undergone a guided-biopsy. The dataset is composed of a total of 19 patients of which 17 patients have biopsy proven CaP and 2 patients are "healthy" with negative biopsies. From those 17, 12 patients have a CaP in the peripheral zone (PZ), 3 patients have CaP in the central gland (CG), 2 patients have invasive

CaP in both PZ and CG. An experienced radiologist has segmented the prostate organ — on T_2-W-MRI, DCE-MRI, and apparent diffusion coefficient (ADC)-MRI — as well as the prostate zones — i.e., PZ and CG —, and CaP on the T_2-W-MRI.

The full description as well as the data set can be found at [8] and are also available through the I2Cvb website.

Our mp-MRI CAD system consists of seven different steps: pre-processing, segmentation, registration, feature detection, feature balancing, feature selection/extraction, and finally classification.

A. Pre-processing

Three types of pre-processing are used for MRI images: (i) noise filtering, (ii) bias correction, and (iii) standardization/normalization. Normalization is, a crucial step to reduce the inter-patient variations which allows to improve the learning during the classification stage. Normalization to pre-process T_2-W-MRI was done following the method [9] and DCE-MRI using [8]. Regarding the ADC map normalization, the probability density function (PDF) within the prostate does not follow a known distribution and thus one cannot use a parametric model to normalize these images and a non-parametric piecewise-linear normalization [10] is the best option for this case. The MRSI modality has been pre-processed to correct the phase, baseline, and frequency [8].

B. Segmentation and registration

For this work, no segmentation method has been developed and the manual segmentation given by our radiologist has been used. The prostate is suffering, however, from a misalignment between the different MRI modalities. Therefore, three registrations have been developed to: (i) the patient motion during the DCE-MRI acquisition, (ii) the patient motion between the T_2-W-MRI and the DCE-MRI acquisitions, and (iii) the patient motion between the T_2-W-MRI and the ADC map acquisition.

C. Feature detection

a) T_2-W-MRI and ADC map features: Apart of using the normalized intensity, edge- and texture-based features are commonly extracted from T_2-W-MRI and ADC map. The following set of filters characterizing edges have been used: (i) Kirsch, (ii) Laplacian, (iii) Prewitt, (iv) Scharr, (v) Sobel, and (vi) Gabor. Apart of Kirsch filter, the other filters are applied in 3D to get more information using a volume and not a slice, as it is usually done. Additionally, features based on phase congruency are computed [11].

To characterize the local texture, both second-order gray-level co-occurence matrix (GLCM)-based features [12] and rotation invariant and uniform local binary pattern (LBP) [13] are extracted. To encode 3D information, the 13 first Haralick features are computed for the 13 possible directions. For the same reason, the LBP codes are computed for the three-orthogonal-planes of each MRI volume.

Note that all these features are extracted at each voxel of the volume.

b) DCE-MRI features: In brief, the entire enhanced signal, semi-quantitative, and quantitative methods are computed.

c) MRSI features: Three different techniques [14] are used to extract discriminative features: (i) relative quantification based on metabolite quantification, (ii) relative quantification based on bounds integration, and (iii) spectra extraction [8] .

d) Anatomical features: 4 different metrics are computed based on the relative distance to the prostate boundary as well as the prostate center, and the relative position in the Euclidean and cylindrical coordinate systems [15], [16].

D. Feature balancing

solving the problem of imbalanced is equivalent to under- or over-sampling part of the dataset to obtain equal number of samples in the different classes. We used several methods and selected the most efficient for our dataset [8]

E. Feature selection and extraction

Feature selection and extraction are used in the experiment: (i) signal-based data — i.e., MRSI and DCE-MRI — are decomposed using feature extraction methods while (ii) image-based features are selected through different feature selection methods.

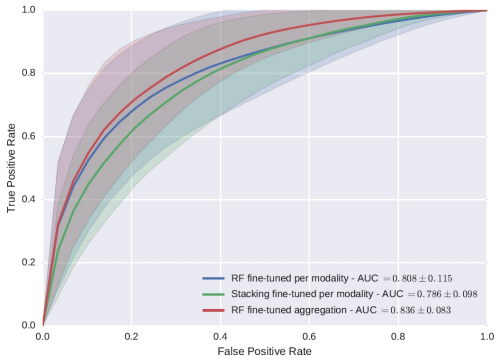

Fig. 1. Analysis of feature combination approaches after fine tuning through balancing and feature selection/extraction.

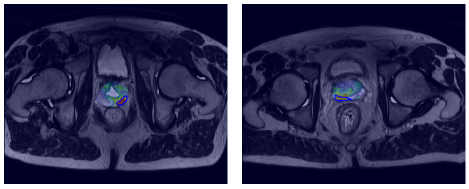

(a) AUC = 0.922 (b) AUC = 0.942

Fig. 2. Illustration the resulting detection of our mp-MRI CAD for CaP detection. The blue contours corresponds to the CaP while the jet overlay represents the probability.

Among those, principal components analysis (PCA), sparse-PCA, and independent components analysis (ICA) are used to decompose signal-based data.

Additionally to feature extraction, two methods of feature selection were used during the experiments. The first feature selection is the one-way analysis of variance (ANOVA) test whereas the second is based on the Gini importance obtained while building our random forest (RF) classifiers.

F. Classification

RF has been chosen as our base classifier — allowing for feature selection as well — to perform classification of individual modality as well as the combination of modalities.

Additionally, we use stacking to create ensemble of base learners using a meta-classifier [17]. AdaBoost (AdB) and Gradient Boosting (GB) are chosen as meta-classifiers to aggregate the base learners in the stacking strategies.

III. Results and Evaluation

Various experiments were run in order to optimize the balancing and the feature selection strategies [8]. We found that once all features are concatenated together, nearmiss-3 (NM-3) [18] is the method providing the best enhancement of the classification performance with an area under the curve (AUC) of 0.824 ± 0.076. Therefore, with this optimal balancing, were here report the final step consisting of three strategies: (i) the selected features from each modality — i.e., 331 features — are concatenated together and used in a RF classifier, (ii) the selected features from each modality — i.e., 331 features — are used to train a stacking classifier with a GB as meta-classifier, and (iii) the selected features from the concatenated set of feature — i.e., 267 features — are used to train a single RF classifier

The experiment was performed in a leave-one-patient-out cross-validation (LOPO CV) fashion and a receiver operating characteristic (ROC) analysis is carried out. The comparative results are shown in Fig. 1. In overall, classification using the fine-tuned features improve the classification performance. The third classification configuration is, however, the one which outperforms others with an AUC of 0.836 ± 0.083. The improvement in terms of AUC is of 0.028 and 0.050 compared with the 1^{st} and 2^{nd}, respectively.

In clinical setting, the AUC score is categorized in 3 levels: (i) "acceptable" discrimination for an AUC ranging from 0.7 to 0.8, (ii) "excellent" discrimination for an AUC ranging from 0.8 to 0.9, and "outstanding" discrimination when the AUC is over 0.9 [19]. Therefore, the combination of all MRI modalities in conjunction with fine-tuning allow to upgrade our CAD system from an "acceptable" to an "excellent" discrimination level.

To illustrate qualitatively the results of our mp-MRI CAD system, 2 diverse examples are presented in Fig. 2 by overlapping the probability map of having a CaP with the original T_2-W-MRI slice.

IV. Conclusion

In this paper, we presented one of the the first CAD system using all the mp-MRI modalities for prostate cancer detection. Indeed, MRSI has nearly never been used together with the other modalities — i.e., T_2-W-MRI, DCE-MRI, and ADC map — apart of the recent work of [20], [21]. With an extensive validation approach to select the best features, the best balancing strategy as well as the best classifier, we obtained results on a rather complicated dataset of 17 patients with an average AUC of 0.836 which put our system among the best, even so different CADs were tested on different datasets.

References

[1] R. Chou, J. M. Croswell, T. Dana, C. Bougatsos, I. Blazina, R. Fu, K. Gleitsmann, H. C. Koenig, C. Lam, A. Maltz, J. B. Rugge, and K. Lin. Screening for prostate cancer: a review of the evidence for the U.S. Preventive Services Task Force. *Ann. Intern. Med.*, 155(11):762–771, Dec 2011.

[2] A. Bourdoumis, A. G. Papatsoris, M. Chrisofos, E. Efstathiou, A. Skolarikos, and C. Deliveliotis. The novel prostate cancer antigen 3 (PCA3) biomarker. *Int Braz J Urol*, 36(6):665–668, 2010.

[3] R. Morgan, A. Boxall, A. Bhatt, M. Bailey, R. Hindley, S. Langley, H. C. Whitaker, D. E. Neal, M. Ismail, H. Whitaker, N. Annels, A. Michael, and H. Pandha. Engrailed-2 (EN2): a tumor specific urinary biomarker for the early diagnosis of prostate cancer. *Clin. Cancer Res.*, 17(5):1090–1098, Mar 2011.

[4] J.Chad Brenner, ArulM. Chinnaiyan, and ScottA. Tomlins. ETS fusion genes in prostate cancer. In Donald J. Tindall, editor, *Prostate Cancer*, volume 16 of *Protein Reviews*, pages 139–183. Springer New York, 2013.

[5] C. M. Hoeks, J. O. Barentsz, T. Hambrock, D. Yakar, D. M. Somford, S. W. Heijmink, T. W. Scheenen, P. C. Vos, H. Huisman, I. M. van Oort, J. A. Witjes, A. Heerschap, and J. J. Futterer. Prostate cancer: multiparametric MR imaging for detection, localization, and staging. *Radiology*, 261(1):46–66, Oct 2011.

[6] C. M. Moore, A. Ridout, and M. Emberton. The role of MRI in active surveillance of prostate cancer. *Curr Opin Urol*, 23(3):261–267, May 2013.

[7] G. Lemaitre, R. Marti, J. Freixenet, J. C. Vilanova, P. M. Walker, and F. Meriaudeau. Computer-aided detection and diagnosis for prostate cancer based on mono and multi-parametric mri: A review. *Computers in Biology and Medicine*, 60:8–31, 2015.

[8] G. Lemaitre. *Computer-Aided Diagnosis for Prostate Cancer using Multi-Parametric Magnetic Resonance Imaging*. PhD thesis, Universitat de Girona and Université de Bourgogne, 2016.

[9] Guillaume Lemaitre, Mojdeh Rastgo Dastjerdi, Joan Massich, Joan C Vilanova, Paul M Walker, Jordi Freixenet, Anke Meyer-Baese, Fabrice Mériaudeau, and Robert Marti. Normalization of t2w-mri prostate images using rician a priori. In *SPIE Medical Imaging*, pages 978529–978529. International Society for Optics and Photonics, 2016.

[10] L. G. Nyul, J. K. Udupa, and X. Zhang. New variants of a method of MRI scale standardization. *IEEE Trans Med Imaging*, 19(2):143–150, Feb 2000.

[11] Peter Kovesi. Image features from phase congruency. *Videre: Journal of computer vision research*, 1(3):1–26, 1999.

[12] R.M. Haralick, K. Shanmugam, and Its'Hak Dinstein. Textural features for image classification. *Systems, Man and Cybernetics, IEEE Transactions on*, SMC-3(6):610–621, 1973.

[13] Timo Ojala, Matti Pietikainen, and Topi Maenpaa. Multiresolution gray-scale and rotation invariant texture classification with local binary patterns. *IEEE Transactions on pattern analysis and machine intelligence*, 24(7):971–987, 2002.

[14] S. Parfait, P.M. Walker, G. Crhange, X. Tizon, and J. Mitran. Classification of prostate magnetic resonance spectra using Support Vector Machine . *Biomedical Signal Processing and Control*, 7(5):499 – 508, 2012.

[15] Li Chen, Zhiqiang Weng, LaiYoong Goh, and Marc Garland. An efficient algorithm for automatic phase correction of {NMR} spectra based on entropy minimization . *Journal of Magnetic Resonance*, 158(12):164 – 168, 2002.

[16] G. Litjens, O. Debats, J. Barentsz, N. Karssemeijer, and H. Huisman. Computer-iided detection of prostate cancer in MRI. *Medical Imaging, IEEE Transactions on*, 33(5):1083–1092, May 2014.

[17] D. H. Wolpert. Stacked generalization. *Neural networks*, 5(2):241–259, 1992.

[18] I. Mani and I. Zhang. knn approach to unbalanced data distributions: a case study involving information extraction. In *Proceedings of Workshop on Learning from Imbalanced Datasets*, 2003.

[19] David W Hosmer Jr and Stanley Lemeshow. *Applied logistic regression*. John Wiley & Sons, 2004.

[20] Rania Trigui, Johel Miteran, Lamia Sellami, Paul Walker, and Ahmed Ben Hamida. A classification approach to prostate cancer localization in 3t multi-parametric mri. In *Advanced Technologies for Signal and Image Processing (ATSIP), 2016 2nd International Conference on*, pages 113–118. IEEE, 2016.

[21] R Trigui, J Mitéran, PM Walker, L Sellami, and A Ben Hamida. Automatic classification and localization of prostate cancer using multi-parametric mri/mrs. *Biomedical Signal Processing and Control*, 31:189–198, 2017.